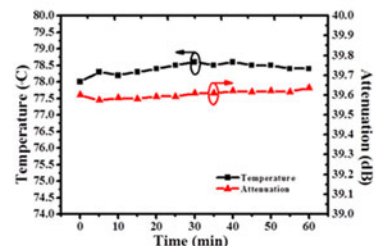


Cladding Light Stripper of High Average Stripped Power Density With High Attenuation of 39 dB and Low Temperature Rise

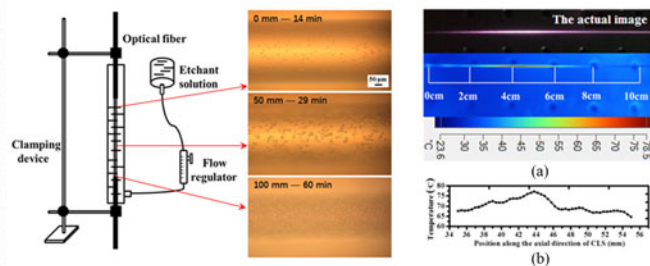
Volume 10, Number 1, February 2018

Shuzhen Zou
Han Chen
Jingyuan Zhang
Haijuan Yu
Zhiyan Zhang
Jing Sun
Xuechun Lin

The two-stage structure cladding light stripper with a high attenuation of 39 dB and good temperature performance.

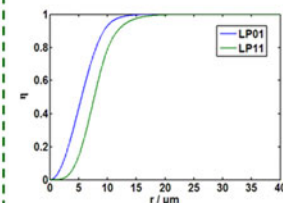


The First Stage



Continuous gradient chemical etching for uniform extraction of the high power scattered cladding light.

The Second Stage



Reducing the cladding diameter to 65 μm to extract the residual low NA cladding light more efficiently without any signal laser loss.

DOI: 10.1109/JPHOT.2017.2785392

1943-0655 © 2017 IEEE

Cladding Light Stripper of High Average Stripped Power Density With High Attenuation of 39 dB and Low Temperature Rise

Shuzhen Zou^{1,2}, Han Chen^{1,2}, Jingyuan Zhang^{1,2,3}, Haijuan Yu^{1,2},
Zhiyan Zhang^{1,2}, Jing Sun^{1,2}, and Xuechun Lin^{1,2}

¹Laboratory of All-Solid-State Light Sources, Institute of Semiconductors, Chinese Academy of Sciences, Beijing 100083, China

²Beijing Engineering Technology Research Center of All-Solid-State Lasers Advanced Manufacturing, Beijing 100083, China

³Department of Physics, Georgia Southern University, Statesboro, GA 30460 USA

DOI:10.1109/JPHOT.2017.2785392

1943-0655 © 2017 IEEE. Translations and content mining are permitted for academic research only. Personal use is also permitted, but republication/redistribution requires IEEE permission. See http://www.ieee.org/publications_standards/publications/rights/index.html for more information.

Manuscript received November 29, 2017; revised December 14, 2017; accepted December 15, 2017. Date of publication December 20, 2017; date of current version January 9, 2018. This work was supported by the National Key R&D Program of China (No. 2016YFB0402201). (Shuzhen Zou and Han Chen contributed equally to this work.) Corresponding author: Xuechun Lin (e-mail: xclin@semi.ac.cn).

Abstract: We demonstrate a 150-mm long cladding light stripper for kW-level operation with high attenuation and low temperature rising. The first 100 mm of the device was designed based on theoretical simulation to achieve uniform extraction of the high-power scattered cladding light and it was constructed by self-developed experimental device for continuous gradient chemical etching. While in the last 50 mm, we reduced the cladding diameter from 400 to 65 μm and then roughed the surface to extract the residual low NA cladding light more efficiently. The power handling capability of this design was tested up to 1.01 kW for an hour stably without causing any damage. The cladding light stripper achieved a high attenuation of 39 dB and a low temperature elevation of 0.05 $^{\circ}\text{C}/\text{input-Watt}$ under the condition of air cooling. The maximum temperature on the surface of the device was only 78.5 $^{\circ}\text{C}$ with an average stripped power density of $7.156 \times 10^6 \text{ W/m}^2$. To the best of our knowledge, the cladding light stripper reported here has the highest average stripped power density and attenuation coefficient without compromising temperature performance. This cladding light stripper is well suitable for application in multikilowatts class fiber lasers.

Index Terms: Fiber laser component, cladding light stripper, double cladding fiber, high power fiber laser.

1. Introduction

Fiber lasers have attracted extensive attention in recent years owing to their rich superiorities, such as high beam quality and high efficiency [1]. Benefited from cladding-pumping technology, the outputs of all-fiber lasers have reached several kW level [2]. But at the output of each amplifier stage, the light remaining in the fiber cladding is hazardous, which not only degrades the beam quality, but also threatens the reliable operation [3]. The unwanted cladding light in a fiber laser system mainly comes from the unabsorbed pump radiation and the leaking signal light due to imperfect splicing, fiber coiling [4] and amplified spontaneous emission [5]. Besides, when a fiber laser is applied to

materials processing, there is a considerable amount of backward propagating radiation coupled into the cladding of the output fiber, which can damage fiber laser components or even the pump laser diodes [6]. To ensure the stability and robustness of a fiber laser system, it is necessary to extract the undesired cladding light.

Cladding light strippers (CLSs) are fabricated for filtering out the cladding light. The temperature performance of the CLS is particularly important in designing a CLS, because severe temperature rising directly limits the power handling capacity and the usability. Also, it is equally important to make a CLS with an attenuation as high as possible, because higher power application requires higher attenuation. To achieve those goals, several fabrication schemes have been proposed [7], [8]. Polymers recoating is a conventional method. Wetter et al. [7] recoated the bare fiber with two polymers having different refractive index, which allowed effective escape of the cladding light. The reported CLS had an attenuation of 30 dB and the temperature reached nearly 55 °C when it stripped 80 W of cladding light with an average stripped power density of the CLS was 1.061×10^6 W/ m². Previous works also proposed a combination of chemical etching technique and polymers recoating [5], [9]. The CLS presented in [9] achieved power handling capability of above 1 kW and attenuation of 26.59 dB with a total length of 1.5 m by combining a fiber-etched CLS with a cascaded polymer-recoated CLS. And the average stripped power density of the CLS was 1.389×10^6 W/ m². Due to the weak thermal aging resistance and low thermal damage threshold of polymers, a CLS with the polymers recoating needs to take full account of heat dissipation for reliable high-power operation, which is always achieved by increasing the length of CLS but leads to low compactness [6].

The CLSs of polymer-free-type have also received a great deal of attention. Using soft metals such as sheets of indium as absorbers for stripping cladding light was reported by Babazadeh et al [10]. This kind of CLS was tested with cladding light of 150 W and the attenuation was 12.4 dB with an average stripped power density of 3.410×10^6 W/ m². The highest temperature was 36 °C on the surface of the device. Besides, some groups applied the laser surface processing technique for guiding the cladding light out [6], [11], [12]. Boyd et al. [11], [12] used a CO₂ laser to generate periodic ablation channels on fiber cladding surface and when a laser power of 300 W was stripped, the temperature on the fiber surface rose to 80 °C with cladding light loss of 20 dB for an average stripped power density of about 3.410×10^6 W/ m². Berisset et al. [13] presented a CLS made by using a UV laser for the micro-machining on the fiber cladding surface. This CLS was tested with cladding power of less than 50 W, which exhibited a temperature rising of 1 °C/ input-Watt and an attenuation of 15.2 dB with an average stripped power density of the CLS was 0.796×10^6 W/ m². Yet, these CLSs based on laser processing technique all relied on fine-adjusted optical and mechanical systems. An alternative method to fabricate the microstructure on the fiber cladding surface is to use surface chemical etching [14], [15], [16]. Kliner et al. [15] applied glass etching paste to create a scattering surface for extracting the cladding light. The CLS demonstrated a stripping efficiency of 27 dB and power handling capability of 500 W, whose average stripped power density was 2.210×10^6 W/ m². Lu Yin et al [16] fabricated a two-segment etched fiber with cladding light attenuation of 19.8 dB and power handling capability of 670 W. And the average stripped power density of the CLS was about 6.747×10^6 W/ m². However, when a CLS is used to handle a cladding power up to kilowatt-level, further careful design of the stripping structure is needed for higher attenuation and more heat dissipation.

In this paper, we worked out a compact kW-level CLS of 150-mm long by combining two different stripping structures. The first stripping structure of the CLS was dealt with gradual chemical etching, in which the chemical etching time was approximately varied continuously along the axial direction of the fiber and thus the fiber surface roughness was smoothly increased as a function of the fiber length. This allowed uniform attenuation of cladding light per surface area and maximized uniformity of the temperature distribution on the fiber surface. The second stripping structure was fabricated to enhance the total attenuation of the cladding light, in which cladding diameter reduction and surface roughing were combined to extract the residual cladding light more efficiently with a low NA. When the stripped power was up to 1.01 kW, the cladding light attenuation was 39 dB and the average stripped power density was 7.156×10^6 W/ m² within the 150-mm long CLS. And the maximum temperature on the surface of the device was 78.5 °C with a temperature elevation rate of 0.05 °C/ input-Watt under the condition of air cooling at room temperature. To the best of our knowledge,



Fig. 1. Schematic illustration of the two-stage stripper. The first stage of the CLS was dealt with gradual chemical etching. The second stage was fabricated by reducing cladding diameter and roughing the fiber surface.

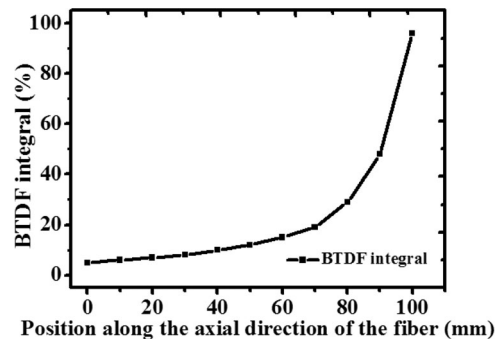


Fig. 2. The normalized values distribution of the BTDF integral along the axial direction of the fiber.

the kW-level CLS reported here has the highest average stripped power density and attenuation coefficient without compromising temperature performance. A stability test was performed for one-hour and the temperature and the residual output power showed no significant fluctuation.

2. Theoretical Design of the CLS

The schematic illustration of the two-stage structure cladding light stripper is described in Fig. 1. The fiber used in the CLS was a double-cladding fiber produced by Nufern with a 20 μm diameter, 0.06 NA core and a 400 μm diameter, 0.46 NA inner cladding.

In order to achieve uniform illumination of the scattered cladding light on the first stage of the CLS, we calculated the scattering rate distribution along the axial direction of the fiber. A model was developed by a commercial ray-tracing software package TracePro. The bidirectional scattering distribution function (BSDF) is used to describe the physical scattering properties of the surface, which is a measurement of the scattering intensity of light from all directions on the surface of an object. BSDF includes the bidirectional reflectance distribution function (BRDF) and the bidirectional transmission distribution function (BTDF).

A fiber geometry with the same structure and refractive index as used in experiments (a cladding diameter of 400 μm , a NA of 0.46 and a length of 100 mm) was established in the model. The 100-mm long fiber was divided into isometric fractions. The light source in the model was set to be flat-topped according to the experiment test. The beam diameter and NA were also the same as the experimental ones.

The surface scattering characteristic parameters of the fiber were constantly adjusted and substituted from the fiber surface characteristic database established in the model. Eventually, we obtained the optimized BTDF integral distribution along the axial direction of the fiber. The normalized values of the BTDF integral were shown in Fig. 2. Fig. 3 shows that the illumination of scattering light is distributed uniformly along the axial direction.

The scattering rate of a fiber surface was determined by the surface characteristics which were directly related to the chemical etching time. We then established the relationship between the scattering rate in the simulation model and the real chemical etching time. The fibers with a coating-free length of 100 mm were uniformly etched for 10 min to 60 min, respectively. The stripped power as a function of fiber length for three typical chemical etching times (10 min, 30 min and 45 min) was provided in Fig. 4. The stripped power evenly increased with the etched length for a mild chemical

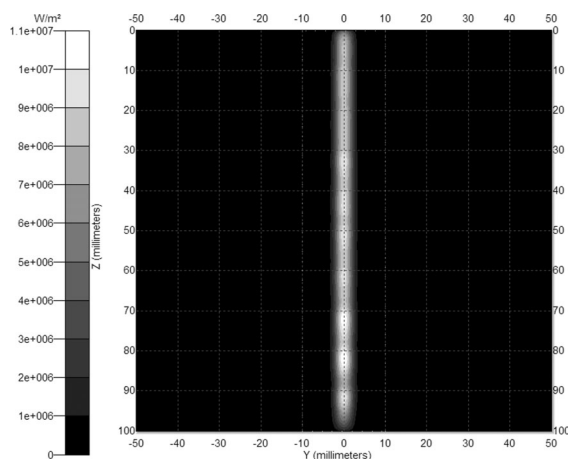


Fig. 3. The illumination distribution of the scattered cladding light in the first stage of the CLS. The illumination of fiber scattering light is distributed uniformly along the axial direction.

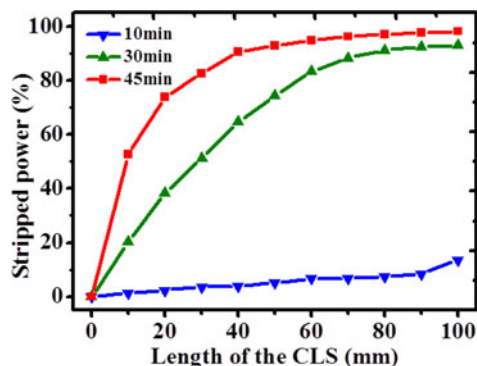


Fig. 4. The stripping capability as a function of the etched lengths with various chemical etching times ranging from 10 min to 45 min.

etching but achieving a low attenuation coefficient (chemical etching time of 10 min). While for the moderate and severe etched fiber (chemical etching time of 30 min and 45 min), the stripped power of the fiber significantly increased at the beginning of 20 mm length.

After establishing another model of a 100 mm fiber with the same structure and refractive index as used in experiments, we calculated the stripped power curves as a function of the fiber length for different scattering rates ranging from 2% to 98%. The stripped power curves as a function of the fiber length for different chemical etching times ranging from 10 min to 60 min were also obtained in the above experiments. We could compare the similarity of the stripped power curves between different the scattering rates and different chemical etching times. Then, the chemical etching times corresponding to the fiber scattering rates (the values of BTDF integral) illustrated in Fig. 2 were obtained and the axial chemical etching time distribution as a function of position in the first stage of CLS is shown in Fig. 5.

The model used for the second stage with 50 mm long fiber was also developed in the TracePro software, in which the scattering rate was set to be 90%, which corresponded to a chemical etching time of about 45 min. The calculations showed that the total attenuation of the CLS was higher than 30 dB when the fiber diameter in the second stage was reduced to 80 μm .

Considering that if the thickness of the cladding was very thin, it would influence the radiation propagating in the fiber core, we calculated the radial power distribution of the fiber core modes in the cladding and obtained the minimum fiber cladding thickness. There are two propagation modes, including LP_{01} mode and LP_{11} mode in a 20 μm fiber core with a NA of 0.06. The radial normalized

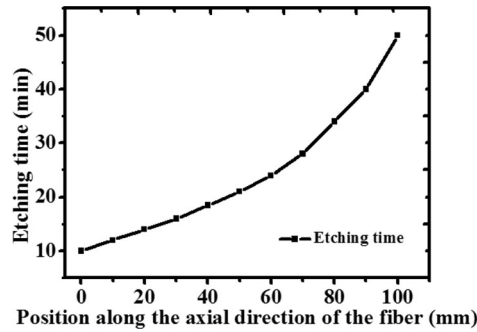


Fig. 5. The simulated chemical etching time distribution of the first stage of the CLS designed by the ray-tracing.

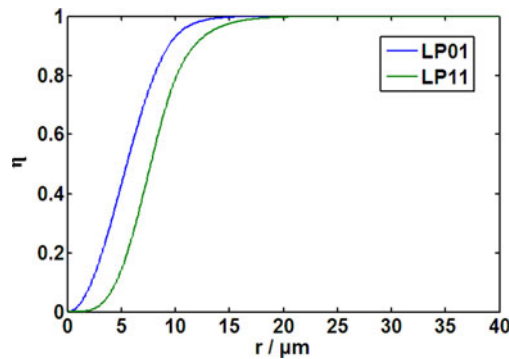


Fig. 6. Radial normalized power distribution of the LP₀₁ mode and the LP₁₁ mode in 20/400 μm (NA = 0.06/0.46) double-cladding fiber.

power η of the LP_{lm} mode within the radius r could be deduced and expressed as following formula:

$$\eta = \begin{cases} \frac{2U^2 K_l^2(W)}{a^2 V^2 J_l^2(U)} \cdot \frac{\int_0^r J_l^2\left(\frac{Ur}{a}\right) r dr}{K_{l-1}(W) K_{l+1}(W)} & (0 \leq r \leq a) \\ 1 - \frac{U^2}{V^2} \left[1 - \frac{K_l^2(W)}{K_{l-1}(W) K_{l+1}(W)} \right] + \frac{2U^2}{a^2 V^2} \cdot \frac{\int_a^r K_l^2\left(\frac{Wr}{a}\right) r dr}{K_{l-1}(W) K_{l+1}(W)} & (r > a) \end{cases} \quad (1)$$

where a is the core radius of the fiber, U and W are transverse propagation coefficient of light field, V is normalized frequency and $V^2 = U^2 + W^2$. J_0 , J_1 and J_2 are the zero-order, the first-order and the second-order Bessel functions, respectively. K_0 , K_1 and K_2 are the zero-order, the first-order and the second-order modified Bessel functions, respectively. According to the result of calculation as shown in Fig. 6, the signal laser loss in the fiber core caused by reducing fiber cladding could be neglected when the fiber diameter is larger than 40 μm (the cladding thickness of 10 μm). The above simulation results offer the theoretical guidance and initial reference to the actual construction.

3. Experimental Design and Results

The preparation setup designed for continuous gradient chemical etching of the first stage is illustrated in Fig. 7. First, the coating of the fiber was stripped in the middle of the fiber with a stripped length of 100 mm. Then the fiber was inserted into the etching tube which had a hole at the bottom center. The tube acted as the etchant solution container and was labeled with a tape measure. Two ends of the fiber were secured by two clamps to suspend the fiber in the tube. After the fiber was finely adjusted, the center hole at the bottom was sealed with wax. KHF₂ etchant solution

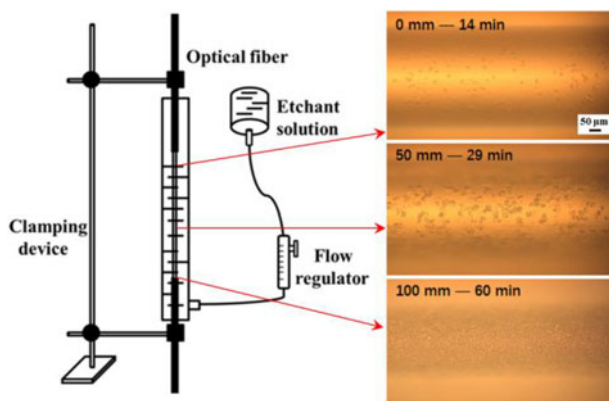


Fig. 7. Schematic setup for the fabrication of a CLS to provide a continuous gradient chemical etching process and the microscopic photographs of the first stage of the CLS at three different positions of 0 mm, 50 mm and 100 mm (corresponding to the chemical etching times of 14 min, 29 min and 60 min, respectively) with the magnification of 200.

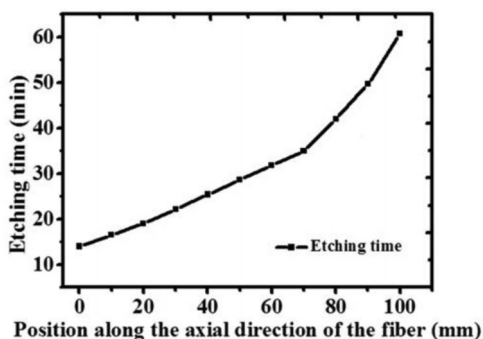


Fig. 8. The experimental chemical etching time distribution of the first stage of the CLS.

was used to fabricate the microstructure on the fiber surface of CLS. The react of the KHF_2 acidic fluoride solution with silicon oxide of fiber generated insoluble silicofluoride-crystals which strongly adhered to the fiber surface and led to light scattering. The etchant solution KHF_2 (0.1 g/ml) was injected from the bottom of the tube through a flow regulator when the experimental environment temperature was 20 °C. The flow regulator was programmed to control the flow setting. The flow setting and the inner-diameter of the tube combined to determine the rising speed of the etching solution, which was expressed as chemical etching time gradient. Changing the combination of two parameters would yield desired chemical etching time gradients. Thus, we could realize the continuous gradient chemical etching and control the chemical etching time distribution along the axial direction of the fiber for given cladding light parameters. The microscopic photographs of the first stage achieved at three different positions with the magnification of 200 are also shown in Fig. 7. The positions of 0 mm, 50 mm and 100 mm along the axial direction of CLS correspond to the chemical etching times of 14 min, 29 min and 60 min, respectively. The particle density on the surface of the etched fiber increases with the chemical etching time.

Experimentally, the chemical etching time was initially set using the simulated results in Fig. 5. Then we made some necessary corrections to the etching time distribution of the first stage according to the actual stripping performance. We obtained a continuous gradient etching stripper based on the optimized axial etching time distribution as shown in Fig. 8 by controlling rising speed of the etching solution.

The experimental setup for testing stripping capability is shown in Fig. 9. We used a homemade 7×1 fiber combiner to combine seven LDs and to achieve a test laser power of above 1 kW. The combined output laser with a NA around 0.46 was then coupled into the CLS. In order to investigate

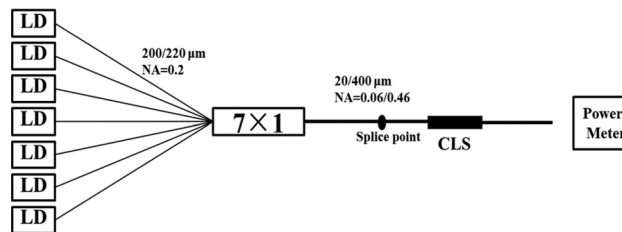


Fig. 9. Schematic experimental setup for testing stripping capability, including seven LDs, a 7×1 fiber combiner (input fibers: $200/220 \mu\text{m}$, $\text{NA} = 0.22$; output fiber: $20/400 \mu\text{m}$, $\text{NA} = 0.06/0.46$), and a CLS under test.

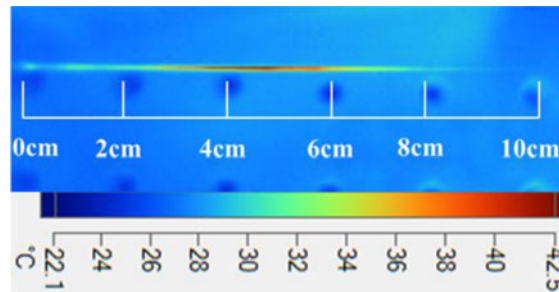


Fig. 10. The thermal image of the CLS with continuous gradient chemical etching time distribution with the test power of 305 W and $\text{NA} = 0.46$. The maximum temperature was $42.5 \text{ }^\circ\text{C}$.

the temperature distribution of the CLS, the stripping section of the CLS was cooled with a small cooling fan, whose area and air flow were $120 \text{ mm} \times 120 \text{ mm}$ and $2.0 \text{ m}^3/\text{min}$, respectively. The CLS was suspended in the center of the fan ventilation area and the distance between them was 20 mm. The cooling fan using in the experiment ensured a relatively constant ambient temperature of about $20 \text{ }^\circ\text{C}$ in environment. The temperature distribution of the CLS was monitored by a thermal camera (Fluke Ti400, whose range was $-40 \text{ }^\circ\text{C} \sim +200 \text{ }^\circ\text{C}$ and the resolution is $0.1 \text{ }^\circ\text{C}$.)

When the input power was 305 W, the highest local temperature of the first stage of the CLS was $42.5 \text{ }^\circ\text{C}$ and an attenuation coefficient of 11 dB was achieved. Fig. 10 presents the thermal distribution of the continuous gradient etched stripper when the stripped laser power amounts to 280 W. The thermal image shows that the heat load can spread out along the stripping section and it is proved that the designed continuous gradient etched fiber stripper can reduce the local high temperature and the thermal damage, which easily occur in uniformly etched or stepped etched stripper when it works at even higher power.

To improve the cladding power attenuation ability, we extended the length of the CLS to fabricate the second stage of the CLS. In the second stage, we reduced the diameter of the fiber by using HF acid. The fiber was corroded and generated a 40-mm uniform-waist and two 5-mm symmetrical conic taper parts shown in Fig. 1. We selected a uniform-waist diameter of $65 \mu\text{m}$ for the purpose of higher stripping efficiency. And the fiber cladding thickness was $22.5 \mu\text{m}$. Then uniform chemical etching was done on the second stage with a chemical etching time of 45 min so that the cladding light of low NA could have a large scattering rate per unit distance. Benefiting from the conic configuration, the cladding light was not stripped by a sudden area mismatch, which avoided the localized heating in the initial part of the second stage.

In order to demonstrate that the CLS configuration did not affect the signal laser in the fiber core, we established a test system as showed in Fig. 11 for measuring the signal laser loss. A 30 W Yb-doped fiber laser pumped by a 976 nm LD was used as the test source, whose output fiber was same type as the one of CLS. The 1080 nm signal laser was obtained behind a 45° dichroic mirror (reflectivity of 98% at 976 nm and transmission of 98.5% at 1080 nm) which was used to filter out the residual pump light. A signal laser transmission of 99.2% was achieved by calculating the

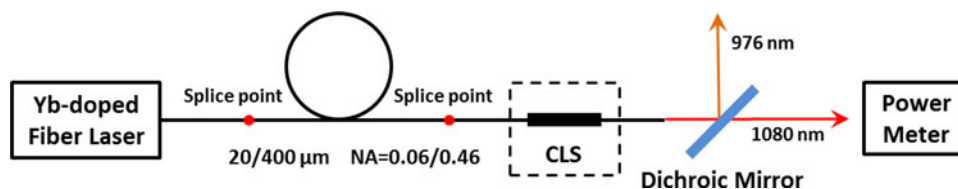


Fig. 11. Schematic experimental setup for measuring the signal laser loss of the CLS.

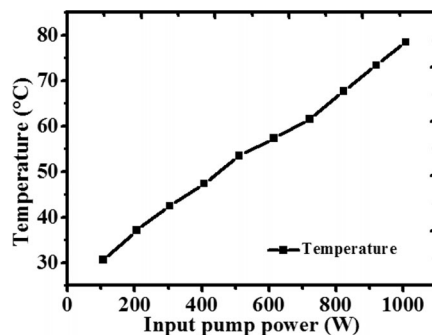


Fig. 12. The temperature elevation of the fiber surface versus input pump power. The highest temperature on the fiber surface rises steadily with a low temperature rising gradient of $0.05\text{ }^{\circ}\text{C}/\text{input-Watt}$.

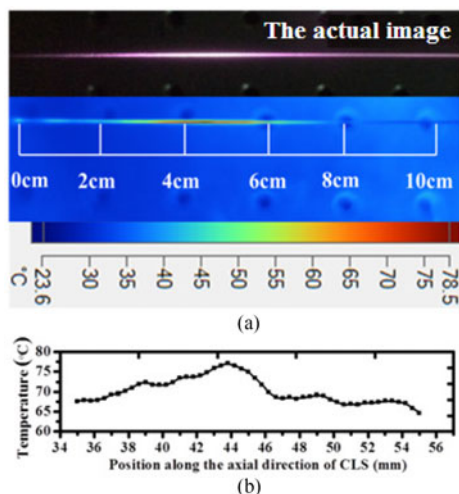


Fig. 13. The thermal image (a) and temperature distribution (b) of the CLS when a laser diode power up to 1 kW was stripped. The maximum recorded temperature was $78.5\text{ }^{\circ}\text{C}$ on the first stage.

ratio of the 1080 nm output power behind the spliced CLS to the 1080 nm output power without the spliced CLS. The average core splicing loss between the output fiber and the CLS was measured to be 0.08 dB. So, if the stripped power of the leaking signal laser in fiber cladding was taken account of, the signal laser transmission of CLS could be close to 100%. This CLS configuration had no influence on the signal laser in the fiber core, which agreed well with theoretical calculation.

To test the performance of the CLS for kW application, a pumping power as high as 1.01 kW was launched into the fiber, and 115 mW residual laser power was detected after the 150-mm long CLS, which corresponded to an average stripped power density of $7.156 \times 10^6\text{ W}/\text{m}^2$ and a total attenuation coefficient of 39 dB. The highest temperature which occurred on the fiber surface of the first stage rose almost linearly with the input pump power and the temperature rising rate was only $0.05\text{ }^{\circ}\text{C}/\text{input-Watt}$ as shown in Fig. 12. Fig. 13(a) showed that when the laser diode power

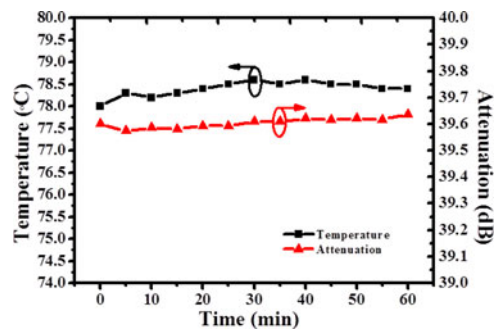


Fig. 14. The temperature and attenuation stability results of the CLS when a laser diode power up to 1 kW was stripped.

up to 1 kW was stripped, the highest temperature of the first stage of the CLS was 78.5 °C. The main temperature rising occurred in the 3.5 cm to 5.5 cm region and the temperature distribution is illustrated in Fig. 13(b). The temperature of the second stage remained slightly higher than the room temperature. One hour stability test under the stripped power of 1.01 kW was performed and the results are given in Fig. 14. The highest temperature fluctuation was $\pm 0.5\%$ and the power attenuation fluctuation was $\pm 0.7\%$. The CLS was packaged in a metal heat sink in the real application and it worked stably without any problem testing under a stripped power of 1.01 kW.

4. Conclusion

We have fabricated a 150-mm long CLS for kW-level operation with high attenuation and low temperature rising by combining two different stripping structures. The device is well suitable for cladding light extraction for several kilowatts class fiber lasers and amplifiers. The experimental characterization showed that the CLS fabricated with such a unique design exhibited a 0.05 °C/W input-Watt temperature rising rate under the condition of air cooling and the maximum temperature of device was 78.5 °C when the stripped power was up to 1.01 kW. The average stripped power density of the whole CLS was 7.156×10^6 W/m². An excellent power attenuation reaching 39 dB was also achieved. The CLS had high temperature stability and power attenuation stability when stripping the cladding light power of 1.01 kW. The performance of the CLS showed here can be further improved through optimizing the chemical etching time arrangement.

References

- [1] D. J. Richardson, J. Nilsson, and W. A. Clarkson, "High power fiber lasers: Current status and future perspectives," *J. Opt. Soc. Amer. B*, vol. 27, no. 11, pp. 63–92, 2010.
- [2] M. H. Muendel *et al.*, "Fused fiber pump and signal combiners for a 4-kW ytterbium fiber laser," *Proc. SPIE*, vol. 7914, 2011, Art. no. 791431.
- [3] R. Poozesh *et al.*, "A novel method for stripping cladding lights in high power fiber lasers and amplifiers," *J. Lightw. Technol.*, vol. 30, no. 20, pp. 3199–3202, Oct. 2012.
- [4] J. Koplów, D. Kliner, and L. Goldberg, "Single-mode operation of a coiled multimode fiber amplifier," *Opt. Lett.*, vol. 25, no. 7, pp. 442–444, 2000.
- [5] Y. Xiao, F. Brunet, M. Kanskar, M. Faucher, A. Wetter, and N. Holehouse, "1-Kilowatt CW all-fiber laser oscillator pumped with wavelength-beam-combined diode stacks," *Opt. Exp.*, vol. 20, no. 3, pp. 3296–3301, 2012.
- [6] S. Boehme *et al.*, "CO₂ laser-based coating process for high power fiber application," *Proc. SPIE*, vol. 8968, 2014, Art. no. 89680Z.
- [7] A. Wetter, M. Faucher, and B. Sevigny, "High power cladding light stripper," *Proc. SPIE*, vol. 6873, 2008, Art. no. 687327.
- [8] W. Guo, Z. Chen, H. Zhou, J. Li, and J. Hou, "Cascaded cladding light extracting strippers for high power fiber lasers and amplifiers," *IEEE Photon. J.*, vol. 6, no. 3, Jun. 2014, Art. no. 1501106.
- [9] P. Yan *et al.*, "Kilowatt-level cladding light stripper for high-power fiber laser," *Appl. Opt.*, vol. 56, no. 7, pp. 1935–1939, 2017.

- [10] A. Babazadeh *et al.*, "Robust cladding light stripper for high-power fiber lasers using soft metals," *Appl. Opt.*, vol. 53, no. 12, pp. 2611–2615, 2014.
- [11] K. Boyd *et al.*, "CO₂ laser-fabricated cladding light strippers for high-power fiber lasers and amplifiers," *Appl. Opt.*, vol. 55, no. 11, pp. 2915–2920, 2016.
- [12] K. Boyd *et al.*, "Advances in CO₂ laser fabrication for high power fibre laser devices," *Proc. SPIE*, vol. 9728, 2016, Art. no. 972838.
- [13] M. Berisset, L. Lebrun, M. Faucon, R. Kling, J. Boulet, and C. Aguegaray, "Laser surface texturization for high power cladding light stripper," *Proc. SPIE*, vol. 9730, 2016, Art. no.973014.
- [14] W. Wang, J. Leng, J. Cao, S. Guo, X. Xu, and Z. Jiang, "Method for stripping cladding light in the high power fiber laser," *Opt. Commun.*, vol. 287, pp. 187–191, 2013.
- [15] A. Kliner *et al.*, "Fabrication and evaluation of a 500 W cladding-light stripper," *Proc. SPIE*, vol. 8616, 2013, Art. no. 86160N.
- [16] L. Yin, M. Yan, Z. Han, H. Wang, H. Shen, and R. Zhu, "High power cladding light stripper using segmented corrosion method: Theoretical and experimental studies," *Opt. Exp.*, vol. 25, no. 8, pp. 8760–8776, 2017.